



University of Richmond
UR Scholarship Repository

Math and Computer Science Faculty Publications

Math and Computer Science

5-2017

A unified inter-host and in-host model of antibiotic resistance and infection spread in a hospital ward


Lester Caudill

University of Richmond, lcaudill@richmond.edu

Barry Lawson

University of Richmond, blawson@richmond.edu

Follow this and additional works at: <http://scholarship.richmond.edu/mathcs-faculty-publications>

 Part of the [Mathematics Commons](#), and the [Medicine and Health Sciences Commons](#)

This is a pre-publication author manuscript of the final, published article.

Recommended Citation

Caudill, Lester and Barry Lawson. "A unified inter-host and in-host model of antibiotic resistance and infection spread in a hospital ward." *Journal of Theoretical Biology* 421 (May 2017): 112–126. doi.org/10.1016/j.jtbi.2017.03.025.

This Post-print Article is brought to you for free and open access by the Math and Computer Science at UR Scholarship Repository. It has been accepted for inclusion in Math and Computer Science Faculty Publications by an authorized administrator of UR Scholarship Repository. For more information, please contact scholarshiprepository@richmond.edu.

A unified inter-host and in-host model of antibiotic resistance and infection spread in a hospital ward

Lester Caudill*, Barry Lawson

*Department of Mathematics and Computer Science, University of Richmond, Virginia
23173 USA*

Abstract

As the battle continues against hospital-acquired infections and the concurrent rise in antibiotic resistance among many of the major causative pathogens, there is a dire need to conduct controlled experiments, in order to compare proposed control strategies. However, cost, time, and ethical considerations make this evaluation strategy either impractical or impossible to implement with living patients. This paper presents a multi-scale model that offers promise as the basis for a tool to simulate these (and other) controlled experiments. This is a “unified” model in two important ways: (i) It combines inter-host and in-host dynamics into a single model, and (ii) it links two very different modeling approaches – agent-based modeling and differential equations – into a single model. The potential of this model as an instrument to combat antibiotic resistance in hospitals is demonstrated with a numerical example.

Keywords: Mathematical models, Antibiotic resistance, Nosocomial infection, Differential equations, Agent-based models

2010 MSC: 92C60, 92C50

1. Introduction

Untested infection control protocols are of dubious value in clinical medicine, and yet, assessing the effectiveness of control measures remains difficult. This is

*Corresponding author
Email address: lcaudill@richmond.edu (Lester Caudill)

particularly true of strategies to prevent or control hospital-acquired infections
5 (HAI). HAIs, while not a new problem, have re-emerged as a major public health
issue in recent years. Elimination of HAIs is an important healthcare priority,
both at the national level and within individual hospitals [1]. The U.S. Centers
for Disease Control and Prevention (CDC) report that there were an estimated
722,000 HAIs in U.S. acute care hospitals in 2011, resulting in about 75,000
10 deaths [2]. The problem is compounded by pathogen populations that have
evolved increased tolerance for the antimicrobials normally used to control them.
Antibiotic resistance (AR) makes HAIs more difficult to clear, by requiring
higher (and possibly more-dangerous) doses of antibiotics. Additionally, AR
can grant pathogens the ability to exist for longer periods of time in the local
15 environment, thereby providing additional opportunities to cause infection. AR
stands as a significant health challenge in its own right, responsible, according
to CDC estimates, for at least two million infections and at least 23,000 deaths
in the U.S. each year [3].

A number of measures to control the appearance and rise of antibiotic re-
20 sistance among the pathogens responsible for HAIs have been proposed. Many
of these measures involve some form of management of antimicrobial use in the
hospitals, both at the administrative level (e.g. by specifying which antimicro-
bials are available to a hospital's prescribing physicians) and in the management
(e.g. drug and dosage selection, monitoring of progress) of individual patient
25 infections. These control measures are predicated on the well-supported idea
that the use of antimicrobial agents can potentially exert an important selective
force that favors AR-mutations within a pathogen population. The connection
between antibiotic use and AR pathogens has been suspected for almost as long
as antibiotics have been in use. In fact, in his Nobel lecture in 1945, Alexander
30 Fleming, a pioneer in antibiotic research, warned of exactly this: "The time may
come when penicillin can be bought by anyone in the shops. Then there is the
danger that the ignorant man may easily underdose himself and by exposing his
microbes to non-lethal quantities of the drug make them resistant." [4]

Ideally, one would evaluate these AR-HAI-control measures through a con-

35 trolled experimental study comparing outcomes in two groups of patients randomized between the current protocol and the new one. However, cost, time, and ethical considerations make this evaluation strategy either impractical or impossible to implement with living patients. Realistic mathematical models, and their implementation as computer-based simulators, can provide valuable tools
40 to conduct *in silico* versions of these controlled experiments, providing valuable insight to hospital epidemiology teams and other decision-making groups. These experiments can be simulated on a large number of virtual patients for many replications, all at minimal cost and in a short period of time, and without the ethical issues that accompany human experimentation. (As of this writing, virtual
45 patients have presented fewer ethical issues, and have proven to be much less litigious than their flesh-and-blood counterparts.)

When considering any mathematical model of AR and HAI dynamics, there are two distinct levels of dynamics that are important to capture. The first, which we will call in-host dynamics, refers to bacterial-level processes that take
50 place inside each individual human host, and includes factors like bacterial population dynamics, changes in resistance due to genetic mutations, pharmacokinetic and pharmacodynamic properties of antibiotics, antibiotic-bacteria interactions, bacterial interactions with the host's immune system, interactions
55 between bacterial strains with different resistance profiles, and so forth. The second level of dynamics, which we will call inter-host dynamics, refers to interactions at the human-level, principally the transfer of bacteria between individuals.

The present work aims to provide a highly realistic model of patient, health-care worker (HCW), bacterial, and antibiotic dynamics as they relate to the rise
60 and spread of antibiotic-resistant HAIs, offering the potential to carefully and systematically test proposed prevention and control strategies and, possibly, to generate new strategies. Our model:

- *combines in-host and inter-host dynamics into a single, unified, realistic model.* The differences in time-scale and dynamics between person-to-

65 person interactions and bacterial growth require different approaches to
modeling the two sets of dynamics, with the further challenge of linking
the two in a practical and realistic way.

- *accurately represents the relationship between AR and HAI.* HAIs will occur even in the absence of AR, but AR will often make an HAI more
70 serious, by making it more difficult, or even impossible, to clear.
- *allows for testing of many different control strategies, including those involving antibiotic-management protocols.* This is accomplished by incorporating many of the treatment parameters, including antibiotic selection, dosage size, mode and frequency of administration, treatment duration,
75 and possible adjustments to existing protocols, as more information (e.g. culture results and resistance profiles) becomes available.
- *naturally includes a heterogeneous population of patients and HCWs in the hospital ward.* The risk of developing an AR-HAI is not uniform across patients, and depends on individual factors such as age, antibiotic-usage
80 history, immunocompetence, colonization state, and co-morbidities. Our model permits heterogeneity in such factors across the patient and HCW population.
- *allows for multiple levels of antibiotic-susceptibility for multiple pathogen species across a wide range of antibiotic classes.* It is a commonly-held
85 misconception that antibiotic resistance is binary, i.e. an individual pathogen is either totally susceptible to or totally unkillable by the antibiotic in question. In reality, a pathogen population will include individuals across a range of different tolerance levels. This is key to the theory that AR-strains arise through natural selection [5].
- 90 • *simulates the appearance of antibiotic-resistant members of pathogen populations via random genetic mutation, with their fates determined by natural selection.* It is unfortunate that popular media continues to characterize

the development of antibiotic-resistance in human pathogens as an intentional retaliatory decision on the part of the bacteria, when, in fact, these
95 microbes are simply going about their lives and trying to survive. It is now widely accepted in the biomedical community that the rise of AR strains within these pathogen populations is primarily due to changes (e.g. use of antibiotics in insufficient concentrations) in the local environment, thereby selecting for these very strains.

- 100 • *allows for multiple colonization and infection statuses within each human.*

We designed our model to reflect the fact that infections and their spread as HAIs depend not only on the pathogens involved, but also the infection's physical location – a skin or upper respiratory infection will spread to another person more readily than, say, a heart valve infection.

- 105 • *incorporates the effects of the immune system response:* The immune response to bacterial infection has a great impact on the course of the infection. In fact, it has been postulated that immunocompromised patients (e.g., the elderly, and patients in oncology wards or transplant wards) may play an important role in the ability of antibiotic-resistant pathogens to
110 survive long-term in hospitals [6].

The balance of this paper is organized as follows: Section 2 discusses related work. The in-host and inter-host models are described in Section 3. Section 4 presents preliminary experiments and results using our model, and Section 5 provides conclusions and future directions.

115 **2. Related Work**

Some efforts have been made to model antibiotic resistance at the in-host level, typically involving standard population dynamics models[7, 8, 9, 10, 11, 12, 13]. Modeling at the inter-host level has received much more attention in the mathematical modeling literature.(See, for example, [14, 15, 16, 17, 18, 19, 20].)
120 By far, the most common approach is to base inter-host infection dynamics

models on the well-established ecologically-based SIR-type models of infectious disease. This approach, made popular by the work of Anderson and May [21], begins by dividing the patient population (and, when included in the model, the HCW population) into a small number of distinct and disjoint categories. 125 The individuals within each category are assumed to be identical to each other in all relevant ways. The model then consists of a system of differential equations (or, less-frequently, a Markov process [22, 23, 24]) designed to describe the rates at which individuals move from one category to another, thereby simulating infection-spread within the patient population. Those researchers who 130 have used models to investigate resistance-control strategies have used infection dynamics models to do so. Most commonly, reports utilizing SIR-type models have assessed hand hygiene [25, 15, 16], patient isolation [15], and various forms of antibiotic restriction/management [25, 14, 26, 20].

The appeal of deterministic SIR-type models stems largely from the potential for theoretical analysis of these models (e.g. the basic reproductive number 135 R_0). In this regard, such infection-spread models have been widely successful. However, in the context of infection dynamics within a hospital ward, this approach is limited by the inherent assumption that the patient (and HCW) population consists of a small number of perfectly homogeneous subgroups, and 140 the consequent assumption that the subgroups are each large enough to justify the use of deterministic (as opposed to stochastic) models to describe the dynamics. While certainly a reasonable approximation in many settings, this is a particular problem for models of a single hospital ward, in which the total number of patients is commonly on the order of 20-50. With numbers this small, 145 individual differences between patients and the effects of randomness are important (as previously noted by other researchers, e.g.[27, 22]), suggesting that a strictly deterministic SIR-type model may not be ideal in the present setting.

Agent-based simulation models offer an attractive alternative for inter-host dynamics, even when the number of hosts is small. The agent-based structure permits the modeler to assign (and modify across time) a different set of 150 attribute-values to each patient and each HCW, allowing full heterogeneity in

the hospital population. Similar to the SIR-model work, most agent-based models of hospital infections focus on simulating control strategies [28, 29, 30, 31, 32]. One recent agent-based approach focuses on community-associated antibiotic resistance [33], an even more challenging problem that requires modeling dynamics throughout the entire community.

There have been some previous efforts at incorporating in-host bacterial resistance levels into models of inter-host interactions. One approach consists of adapting an SIS inter-host model by dividing the infected/colonized population I into two (as in Boni and Feldman [34]) or more (as with Temime and collaborators [35, 36]) sub-populations. Each member of a given sub-population is assumed to carry the same pathogen strain (i.e. the same resistance-level to the antibiotic under consideration), with the sub-populations differing from one another by pathogen strain. The works [35, 36] permit random movement of hosts between the sub-populations, simulating random mutations of pathogens, a widely-accepted source for changes in resistance.

A second approach, used by Stewart et al ([37]) and Webb and collaborators ([38, 39]), permits hosts to carry two pathogen strains (representing different resistance-levels) simultaneously. To incorporate the effects of these multiple strains, these researchers use an inter-host modeling structure similar to the partial differential equations models used in population dynamics, where the in-host influence enters as a new independent variable, representing either the proportion of the resistant strain within the host (in the former) or age-of-infection (as in the latter).

Three other recent works are worth noting here, because, similar in spirit to our work, the authors link an agent-based sub-model with a sub-model of different type and scale into a single model. To investigate effects on MRSA transmission and prevalence, Barnes and collaborators [40] use an agent-based approach to model movement of patients between facilities, and use modified SIR equations to model transmission within each facility. Similarly, Kardaš-Słoma and collaborators [32] link an agent-based model of inter-host hospital dynamics with a differential equations model of inter-host interactions in the

surrounding community. Djanatliev and collaborators [41] use an agent-based approach in the context of mobile stroke units, and model population and disease dynamics using system dynamics. The latter work differs significantly in context, while all three works differ in scope and, relative to our in-host model, in choice of mathematical model and corresponding level of detail.

The two principal contributions of our work are (1) the level of detail and the number of factors incorporated into our differential equations and probabilistic model of in-host bacterial and antibiotic dynamics, and (2) tight integration of this in-host model with agent-based simulation, which naturally models heterogeneous populations and allows for modeling complex interactions at the human level. Recent work comparing differential equations models with agent-based simulation concludes that the former are more tractable and amenable to theoretical analysis, while the latter allow for heterogeneity and complexity [42]. Moreover, a recent call for multi-agent simulation [43] points out that these models provide natural heterogeneity, can be easily combined (bridged) with other types of models, and are well suited for detailed hypothesis testing. Our work is therefore timely and appropriate, allowing for careful combination of two generally disparate approaches, leveraging the advantages of each.

3. Multi-Level HAI Model

We seek to model hospital infection dynamics at multiple levels, from the interaction between patients and HCWs, to in-host processes at the pathogen-level. We will make repeated use of several acronyms, which we summarize for the reader in Table 1.

3.1. Agent-based model of inter-host interactions

An agent-based simulation model is typically defined by three components: (a) a collection of heterogeneous autonomous agents (actors), each having characteristics and behaviors; (b) a collection of rules that define the actions of, and interactions between, agents; and (c) an environment in which the agents reside

Table 1: Acronyms and abbreviations used, including the number of the Section in which it first appears.

Acronym	Description	Section #
HAI	hospital-acquired infections	1
AR	Antibiotic resistance	1
AR-HAI	Antibiotic resistant hospital-acquired infections	1
HCW	Healthcare workers	1
BPV	Bacteria population vector	3.1
IPV	Immune responder population vector	3.1
IC-parameter	Immunocompetence parameter	3.1
C-Cat	Colonization category	3.2
AR-profile	Antibiotic-resistance profile	3.2
MIC	Minimum inhibitory concentration	3.2
HAP	Hospital-acquired pneumonia	4

and with which they interact. In our context, agents are the people represented by the simulation model, i.e., HCWs and patients, and the environment is a single care unit within the hospital. Each agent in our model represents either a single HCW or a single patient, having a set of characteristics (data) with values unique to that agent. These characteristics include:

- two vectors, a *bacteria population vector* (BPV) and an *immune responder population vector* (IPV), respectively characterizing the current bacteria population and current immune responder population within the agent (See Subsection 3.2.);
- a scalar *immunocompetence parameter* (*IC-parameter*) $\lambda > 0$, describing the relative health of the agent’s immune system at the current time (A larger λ reflects a stronger immune system. See Subsection 3.3.);
- blood volume, for computing antibiotic concentrations;
- the antibiotic treatment history for the agent.

In addition, each agent also has a set of behaviors that correspond to the possible actions and interactions of the HCWs and patients. For example, HCW behaviors include visiting patients on rounds and interacting with other health-care workers, while patient behaviors include methods to model interacting with

another patient and receiving antibiotic treatment.

230 Time evolution of the model is implemented using discrete-event (specifically
next-event) simulation [44], where the types of events currently include the fol-
lowing: (a) HCW visiting a patient on rounds; (b) HCW addressing a random
patient call; (c) two HCWs interacting; (d) two patients interacting; (e) appli-
cation of antibiotic to an agent; (f) HCW shift change; and (g) discharge of a
235 patient and admission of a new patient. The simulation progresses by advancing
the simulation clock to the time of the next event to occur in simulated time,
and then handling the details associated with that type of event (from among
the seven types listed above). Whenever an event occurs, the agent-based imple-
mentation invokes appropriate differential equations and probabilistic methods
240 from the in-host model (see Sections 3.2–3.5) to model the bacterial, immune re-
sponder, and immunocompetence dynamics between times of agent-level events.
This combination of agent-based modeling and differential equations modeling
provides realistic heterogeneity not available in typical mathematical models.
Readers interested in further details about the agent-based component of the
245 present model are invited to consult [45].

3.2. Linkage between inter-host and in-host dynamics

The agent-based inter-host model and the differential equations/probabilistic
in-host model (see below) are linked by way of the BPV and, indirectly, by
the IPV. To realistically model the transfer of bacteria between agents, it is
250 necessary to distinguish between different infection states within each agent.
We subdivide each agent’s bacterial population into six *colonization categories*
(*C-Cats*), which reflect six different colonization/infection states that bear on
the spread of person-person bacteria transfer. These six C-Cats, described in
Table 2, represent our efforts to introduce distinctions in a host’s pathogen
255 population in two ways:

- *distinguish between pathogen populations that will trigger an immune re-
sponse and those that will not.* This is usually a question of physical

Table 2: The six colonization/infection categories (C-Cats) used by the model.

C-Cat	Description	Immune Response?	Examples
1	colonization that can be anticipated and addressed	no	hand or equipment colonization
2	unnoticed colonization – no preemptive action taken	no	nasal carriage of <i>S. aureus</i>
3	present as part of the agent’s regular microflora	no	usual gut bacteria
4	can be self-spread, spread directly agent-to-agent, or spread via HCW intervention	yes	skin or respiratory infections
5	can be self-spread or spread via HCW intervention, but not spread directly agent-to-agent	yes	urinary tract infections
6	can be spread via HCW intervention, but not self-spread nor spread directly agent-to-agent	yes	bloodstream infections

location of the pathogen, and the source of the distinction between the terms “colonization” and “infection”. Column 3 in Table 2 indicates which C-Cats trigger an immune response.

- *distinguish between different likelihoods of transmission of a pathogen population from one host to another.* These likelihoods usually depend both on physical location of the pathogen and the nature of the interaction of the host with other (human) agents. (These interactions are discussed in detail in Section 3.4, and are reflected in the transfer matrix in Table 6.)

To reflect this structure, we subdivide each host’s bacteria population into six sub-populations, corresponding to the six C-Cats, as described in Table 2.

As part of the model input, the user specifies the particular bacteria species and antibiotics to be used in the model. If we let J denote the number of bacteria species to use, then, within each of the six C-Cats, the bacteria population is subdivided into J subpopulations, according to species. To capture the dynamics of AR appearance via genetic mutation, it is necessary to further subdivide each of these $6J$ subpopulations according to the possible antibiotic resistance

profiles (AR-profiles). To explain what is meant by “AR-profile”, we first note
 275 that the resistance-level of a bacterial strain with respect to a particular anti-
 biotic can be quantified by the notion of *minimum inhibitory concentration*
 (*MIC*). The MIC is the minimum concentration of the antibiotic at which the
 bacteria strain cannot reproduce. (So, for a given antibiotic, a bacterial strain
 with a larger MIC is considered to be more resistant (or less susceptible) to
 280 that antibiotic than a strain with a smaller MIC.) Commonly, bacterial popu-
 lations are heterogeneous in MIC-value, with respect to a particular antibiotic,
 as reproduction sometimes results in viable genetic mutants with a MIC-value
 that differs from the parent bacterium. We represent this heterogeneity in our
 model by introducing, for each bacteria-antibiotic pair, a discrete set of N MIC-
 285 values. (For simplicity, the same value of N is used for each bacteria-antibiotic
 pair included in the model, although this requirement can be relaxed – see the
 discussion in Section 5) For the pairing of bacteria species j and antibiotic m ,
 this set of MIC-values is determined by first identifying an upper bound μ_{jm}
 on the maximum serum MIC-level for this pairing, then dividing the interval
 290 $(0, \mu_{jm}]$ into $N - 1$ subintervals

$$(\mu_{jm(n-1)}, \mu_{jmn}], \quad n = 1, \dots, N - 1,$$

where $\mu_{jm0} = 0$ and $\mu_{jmN} = \mu_{jm}$. Then, the N possible MIC-values R_{jm1}, \dots, R_{jmN}
 for species j and antibiotic m are set as follows:

$$R_{jmn} = \mu_{jm(n-1)}, \quad n = 2, \dots, N, \quad (1)$$

$$R_{jm1} = \epsilon R_{jm2}, \quad (2)$$

where $0 < \epsilon < 1$. (R_{jm1} is chosen small in order to represent the members of
 species j that are most-susceptible to antibiotic m .)

Denoting the number of antibiotics in the model by M , an individual bac-
 terium from species j will have one MIC-value $R_{j1n_{j1}}$ with respect to antibiotic

Table 3: The possible MIC-values in the case of two bacteria species, two antibiotics, and three resistance-levels per antibiotic. Here, μ_{jm} is an upper bound on the maximum serum concentration of Antibiotic m vs. Bacteria Species j . As a result, Bacteria Species j has nine possible AR-profiles, each of the form {MIC vs. AB1, MIC vs. AB2}: $\left\{\frac{\epsilon\mu_{j1}}{2}, \frac{\epsilon\mu_{j2}}{2}\right\}$, $\left\{\frac{\epsilon\mu_{j1}}{2}, \frac{\mu_{j2}}{2}\right\}$, $\left\{\frac{\epsilon\mu_{j1}}{2}, \mu_{j2}\right\}$, $\left\{\frac{\mu_{j1}}{2}, \frac{\epsilon\mu_{j2}}{2}\right\}$, $\left\{\frac{\mu_{j1}}{2}, \frac{\mu_{j2}}{2}\right\}$, $\left\{\frac{\mu_{j1}}{2}, \mu_{j2}\right\}$, $\left\{\mu_{j1}, \frac{\epsilon\mu_{j2}}{2}\right\}$, $\left\{\mu_{j1}, \frac{\mu_{j2}}{2}\right\}$, and $\{\mu_{j1}, \mu_{j2}\}$.

	Antibiotic 1 (AB1)	Antibiotic 2 (AB2)
Bacteria Species 1	$R_{111} = \frac{\epsilon\mu_{11}}{2}, R_{112} = \frac{\mu_{11}}{2}, R_{113} = \mu_{11}$	$R_{121} = \frac{\epsilon\mu_{12}}{2}, R_{122} = \frac{\mu_{12}}{2}, R_{123} = \mu_{12}$
Bacteria Species 2	$R_{211} = \frac{\epsilon\mu_{21}}{2}, R_{212} = \frac{\mu_{21}}{2}, R_{213} = \mu_{21}$	$R_{221} = \frac{\epsilon\mu_{22}}{2}, R_{222} = \frac{\mu_{22}}{2}, R_{223} = \mu_{22}$

1, one MIC-value $R_{j2n_{j2}}$ with respect to antibiotic 2, and, more generally, one MIC-value $R_{jmn_{jm}}$ with respect to antibiotic m , for $m = 1, \dots, M$. We refer to the resulting sequence

$$\{R_{jmn_{jm}}\}_{m=1}^M$$

295 of M MIC-values as the AR-profile of this bacterium. (Table 3 gives an example of this AR-profile structure.) Noting that there are a total of N^M possible AR-profiles for members of bacterial species j , we now sub-divide each of the J bacterial species into $N^M \equiv K$ sub-populations, according to AR-profile.

To summarize, we separate the bacteria population within an individual
300 human host by the six C-Cats, then by the J bacterial species, then by the K possible AR-profiles, resulting in a total of $6JK$ bacteria sub-populations, which we then organize as the host's bacteria population vector (BPV). If we denote by P_{ijk} the pathogen subpopulation for C-Cat i , species j , and AR-profile k , then P_{ijk} occupies entry $(i-1)JK + (j-1)K + k$ in the BPV.

305 The IPV is organized in a similar fashion to the BPV, except we include only C-Cats 4-6 (See below.), and we impose no sub-division based on AR-profile. This results in an IPV of length $3J$, in which the immune responder sub-population I_{ij} occupies entry $(i-4)J + j$ in the IPV. An illustration of the structure of the BPV and IPV, in the case of two bacteria species, two

Table 4: The components of the BPV and IPV, in the case of two bacteria species, two antibiotics, and two resistance-levels. The rows represent the six C-Cats, while the columns represent the bacteria species, each sub-divided into the four possible AR-profiles. P_{ijk} represents the bacteria sub-population in C-Cat i of bacteria species j , with AR-profile k . I_{ij} is similarly defined, but is not sub-divided by AR-profile. Note that the immune responder populations I_{ij} exist only for C-Cats 4-6.

	Bacteria 1				Bacteria 2			
	AR 1	AR 2	AR 3	AR 4	AR 1	AR 2	AR 3	AR 4
C-Cat = 1	P_{111}	P_{112}	P_{113}	P_{114}	P_{121}	P_{122}	P_{123}	P_{124}
C-Cat = 2	P_{211}	P_{212}	P_{213}	P_{214}	P_{221}	P_{222}	P_{223}	P_{224}
C-Cat = 3	P_{311}	P_{312}	P_{313}	P_{314}	P_{321}	P_{322}	P_{323}	P_{324}
C-Cat = 4	P_{411}	P_{412}	P_{413}	P_{414}	P_{421}	P_{422}	P_{423}	P_{424}
	I_{41}				I_{42}			
C-Cat = 5	P_{511}	P_{512}	P_{513}	P_{514}	P_{521}	P_{522}	P_{523}	P_{524}
	I_{51}				I_{52}			
C-Cat = 6	P_{611}	P_{612}	P_{613}	P_{614}	P_{621}	P_{622}	P_{623}	P_{624}
	I_{61}				I_{62}			

310 antibiotics, and two resistance-levels, is shown in Table 4. For that example, the BPV and IPV have the forms

$$BPV = \{P_{111}, \dots, P_{114}, P_{121}, \dots, P_{124}, P_{211}, \dots, P_{214}, \dots, P_{621}, \dots, P_{624}\},$$

$$IPV = \{I_{41}, I_{42}, I_{51}, I_{52}, I_{61}, I_{62}\}.$$

3.3. Bacterial dynamics within each host

In modeling the time-evolution of the pathogen and immune responder populations (as represented by the BPV and IPV, respectively), we consider three
315 important factors:

1. the natural reproduction and death for the pathogen and immune responder sub-populations,
2. changes to the BPV and IPV due to interactions between the two population types (only relevant for C-Cats 4-6),
- 320 3. the possibility of resistance-altering genetic mutations within newly produced members of the pathogen population.

We model the first two factors differently for C-Cats 1-3 and C-Cats 4-6, because the immune responders only enter into the latter. Specifically, for C-Cat i , $i = 1, 2, 3$, the BPV entry P_{ijk} corresponding to pathogen species j and AR-profile k is assumed to satisfy either exponential or logistic growth i.e.:

$$\frac{dP_{ijk}}{dt} = f_{ijk}(P_{ijk}), \quad P_{ijk}(0) = P_{ijk,0}, \quad (3)$$

for $j = 1, \dots, J$, and $k = 1, \dots, K$, where either

$$f_{ijk}(P_{ijk}) = a_{ijk}P_{ijk} \quad \text{or} \quad f_{ijk}(P_{ijk}) = a_{ijk}P_{ijk} \left(1 - \frac{\sum_{k=1}^K P_{ijk}}{P_{max,ij}} \right).$$

where the sum is over all AR-profiles and $P_{max,ij}$ represents the carrying capacity for bacteria species j in C-Cat i . For $i = 4, 5, 6$, we model the joint evolution of P_{ijk} and the corresponding IPV entry I_{ij} by adapting the immune response model of [46] to the case of multiple AR-profiles:

$$\frac{dP_{ijk}}{dt} = \frac{1}{\lambda} f_{ijk}(P_{ijk}) - \frac{b_{ij}}{\lambda} \frac{P_{ijk} I_{ij}}{K_{ij} + P_{ijk}}, \quad P_{ijk}(0) = P_{ijk,0}, \quad (4)$$

$$\frac{dI_{ij}}{dt} = \frac{\lambda^{\frac{1}{2}} c_{ij} \sum_{k=1}^K P_{ijk}}{B_{ij} + \sum_{k=1}^K P_{ijk}} + \frac{\lambda^{\frac{1}{2}} d_{ij} I_{ij}}{M_{ij} + I_{ij}} - \frac{q_{ij}}{\lambda} I_{ij}, \quad I_{ij}(0) = I_{ij,0}, \quad (5)$$

for $j = 1, \dots, J$, and $k = 1, \dots, K$. The terms on the right-hand side of (4) represent, respectively, pathogen growth/death and removal by the immune response, while the terms on the right-hand side of (5) represent, respectively, pathogen-induced immune response activation, auto-catalytic immune response activation, and natural removal of immune cells. The parameter λ represents the IC-parameter for the host, one of the attributes carried by each agent. (See Section 3.1.) The remaining model parameters in (3)-(5) do not vary between hosts, and are summarized in Table 5. The interested reader is referred to [46] for further details.

Table 5: Definitions of parameters appearing in equations (4)-(5), with subscripts indicating C-Cat i , pathogen species j , and AR-profile k .

Parameter	Description
a_{ijk}	Net per capita pathogen growth rate
b_{ij}	Pathogen death rate due to immune response
K_{ij}	Immune kill rate saturation constant
c_{ij}	Rate of pathogen-induced immune responder activation
B_{ij}	Pathogen-induced immune activation saturation constant
d_{ij}	Rate of autocatalysis-induced immune responder activation
M_{ij}	Autocatalysis-induced immune activation saturation constant
q_{ij}	Immune responder decay rate

340 To realistically reflect the rise and spread of antibiotic-resistant members
of an agent’s bacterial population, our model must also account for the un-
derlying natural selection dynamics within the bacterial subpopulations. Key
to the rise of AR is the occasional appearance of resistant individuals in the
bacterial population, resulting from random genetic mutations occurring dur-
345 ing reproduction of the susceptible bacteria. We accomplish this by expanding
the in-host model (3)-(5) to include a probabilistic component, to allow for the
possibility of bacterial genetic mutations (occurring during reproduction) that
result in a change in a bacterium’s AR-profile. When an agent’s BPV is updated
(via the system (3)-(5)), updating is paused at regular time intervals to allow
350 for some of the newly-created members of the BPV to change from one AR-
profile to another via mutation. Specifically, for each nonzero sub-population,
we draw a pseudo-random deviate from a binomial distribution. These deviates
determine, for each entry in the BPV, how many of the newly-created members
of that sub-population will be moved to different AR-profiles.

355 To illustrate the process of assigning mutants to new AR-profiles, consider
the case of one pathogen species, two antibiotics, and three MIC-levels per
antibiotic. Denoting the MIC-levels with subscripts:

- For antibiotic 1: $R_{11} < R_{12} < R_{13}$,
- For antibiotic 2: $R_{21} < R_{22} < R_{23}$,

360 we represent the nine possible AR-profiles by pairs of the form $\{R_{1i}, R_{2j}\}$, for $i, j \in \{1, 2, 3\}$, and define a metric d on this set of AR-profiles as

$$d(\{R_{1i_1}, R_{2j_1}\}, \{R_{1i_2}, R_{2j_2}\}) = |i_1 - i_2| + |j_1 - j_2|. \quad (6)$$

Then, the bacteria from AR-profile $\{R_{1i}, R_{2j}\}$ selected to mutate are assigned to their new AR-profile by being distributed randomly (with a uniform probability distribution) among all AR-profiles that are exactly one unit (according to the metric in (6) from their original AR-profile. For instance, mutants originating from AR-profile $\{R_{11}, R_{21}\}$ will be distributed between AR-profiles $\{R_{11}, R_{22}\}$ and $\{R_{12}, R_{21}\}$, but no others, while mutants originating from AR-profile $\{R_{11}, R_{22}\}$ will be distributed between AR-profiles $\{R_{11}, R_{21}\}$, $\{R_{11}, R_{23}\}$, and $\{R_{12}, R_{22}\}$. Our code also allows for mutation to AR-profiles that are two units away from the original, but with a much smaller probability.

370

3.4. Bacteria transfer between hosts

Each interaction event between a pair of agents in our model provides an opportunity for those agents to transfer some of their bacteria to each other. Our implementation of this “bacterial exchange” is best described in terms of the six C-Cats from Table 1. In this context, the possible bacterial exchanges between the two types of agents (patient and HCW) are given in Table 6. (Based on an extensive review of the infectious diseases literature, these possible exchanges are widely accepted.)

375

For an interaction event between two agents, A_1 and A_2 , the bacterial exchange between them is treated as a pair of one-way bacterial transfers – one from A_1 to A_2 and the other from A_2 to A_1 . Each of these one-way transfers is a two-step process:

380

1. For each “Y” in the appropriate sub-table from Table 6, we draw a deviate from a Bernoulli probability distribution to determine whether or not

Table 6: Summary of the possible bacterial exchanges between agents. Each row represents one of the C-Cats of the donor agent, and each column represents one of the C-Cats of the recipient agent. Each entry in the table is a list of three letters, corresponding to the three possible transfers between agents – patient-to-HCW, HCW-to-patient, and same-kind (i.e. either patient-to-patient or HCW-to-HCW) – respectively. A “Y” indicates that the transfer is possible, while an “N” indicates that the transfer is not possible.

	C-Cat=1	C-Cat=2	C-Cat=3	C-Cat=4	C-Cat=5	C-Cat=6
C-Cat=1	Y, Y, Y	Y, Y, Y	N, N, N	Y, Y, Y	N, Y, N	N, Y, N
C-Cat=2	Y, Y, Y	Y, Y, Y	N, N, N	Y, Y, Y	N, Y, N	N, Y, N
C-Cat=3	Y, N, N	Y, N, N	N, N, N	Y, N, N	N, N, N	N, N, N
C-Cat=4	Y, Y, Y	Y, Y, Y	N, N, N	Y, Y, Y	N, Y, N	N, Y, N
C-Cat=5	Y, N, N	N, N, N	N, N, N	N, N, N	N, N, N	N, N, N
C-Cat=6	Y, N, N	N, N, N	N, N, N	N, N, N	N, N, N	N, N, N

385 transfer between the two corresponding C-Cats actually occurs.

2. For each positive result from Step 1, a randomly-determined proportion of the bacteria population is moved from the donor agent’s C-Cat to the appropriate C-Cat of the recipient agent.

The probability used for the Bernoulli deviates in Step 1 is based on user-chosen
 390 parameters α (one for each “Y” in Table 6), representing the probability of each transfer during a ten-minute interaction between agents. The probability of transfer for an interaction of duration Δ is computed by the scaling formula

$$\text{transfer probability} = 1 - (1 - \alpha)^{\frac{\Delta}{10}}. \quad (7)$$

To illustrate Step 2, we denote the BPV of agent A_m by $\{P_{ijk}^{(m)}\}$, and suppose that 100q% of the pathogen population is to be transferred from C-
 395 Cat-4 of agent A_1 to C-Cat-5 of agent A_2 . We implement this by adjusting the corresponding BPV entries, as indicated in Table 7.

3.5. Use of antibiotics

When an antibiotic treatment event is initiated for an agent, the user specifies the choice of antibiotic (from the M choices included in the simulation),
 400 dosage, mode of administration (oral, IV, or bolus injection), and number and frequency of doses. This action expands the in-host model (3)-(5) to include, for

Table 7: An illustration of bacterial transfer from one host (Agent 1) to another (Agent 2), in which a proportion q of bacteria species j with resistance profile k is transferred from C-Cat 4 of Agent 1 to C-Cat 5 of Agent 2. Here, $P_{ijk}^{(m)}$ represents the entry of Agent m 's BPV corresponding to C-Cat i , bacteria species j , and resistance profile k .

BPV-entry	BPV-entry before transfer	BPV-entry after transfer
C-Cat 4 of Agent 1	$P_{4jk}^{(1)}$	$(1 - q)P_{4jk}^{(1)}$
C-Cat 5 of Agent 2	$P_{5jk}^{(2)}$	$P_{5jk}^{(2)} + qP_{4jk}^{(1)}$

the treated agent, an additional M dependent variables, $C_m(t)$, representing the concentration, in the bloodstream, of antibiotic m at time t . The time-evolution of each $C_m(t)$ is assumed to be governed by standard pharmacokinetics initial-value problem models [47]. Assuming that the antibiotic affects only C-Cats 3-6, the model equations (3)-(5) remain the same for C-Cats 1 and 2, while the bacterial evolution equations (3) and (4) each gain an additional antibiotic-driven removal term for C-Cats 3-6. So, the in-host model (3)-(5) becomes, for C-Cat i , bacteria species j , AR-profile k , and antibiotic m :

For C-Cats $i = 1, 2$:

$$\frac{dP_{ijk}}{dt} = f_{ijk}(P_{ijk}), \quad (8)$$

for C-Cat $i = 3$:

$$\frac{dP_{ijk}}{dt} = f_{ijk}(P_{ijk}) - P_{ijk} \sum_{m=1}^M d_{ijm} (C_m(t) - \Lambda_{jkm}), \quad (9)$$

and for C-Cats $i = 4, 5, 6$:

$$\frac{dP_{ijk}}{dt} = \frac{1}{\lambda} f_{ijk}(P_{ijk}) - \frac{b_{ij}}{\lambda} \frac{P_{ijk} I_{ij}}{K_{ij} + P_{ijk}} - P_{ijk} \sum_{m=1}^M d_{ijm} (C_m(t) - \Lambda_{jkm}) \quad (10)$$

$$\frac{dI_{ij}}{dt} = \frac{\lambda^{\frac{1}{2}} c_{ij} \sum_{k=1}^K P_{ijk}}{B_{ij} + \sum_{k=1}^K P_{ijk}} + \frac{\lambda^{\frac{1}{2}} d_{ij} I_{ij}}{M_{ij} + I_{ij}} - \frac{q_{ij}}{\lambda} I_{ij}, \quad (11)$$

for $j = 1, \dots, J$, and $k = 1, \dots, K$. Here, Λ_{jkm} is the MIC, with respect to antibiotic m , of the subpopulation of bacteria species j with AR-profile k . The
 415 function d_{ijm} is a saturating threshold function of the form

$$d_{ijm}(y) = \begin{cases} 0, & y \leq 0, \\ \frac{\alpha_{ijm} y}{\beta_{ijm} + \gamma_{ijm} y}, & y > 0, \end{cases} \quad (12)$$

where α_{ijm} , β_{ijm} , and γ_{ijm} are positive constants. Two observations, regarding the antibiotic-induced removal term in (9) and (10):

- The piecewise structure of (12) causes the antibiotic to affect a particular bacterial subpopulation P_{ijk} only when the antibiotic concentration $C_m(t)$
 420 exceeds the MIC Λ_{jkm} for that subpopulation. Moreover, the effect depends on the extent to which $C_m(t)$ exceeds the associated MIC, through the term $C_m(t) - \Lambda_{jkm}$.
- The sum over m makes it possible to model situations in which an agent is being treated with two or more antibiotics, either concurrently or in close
 425 succession.

3.6. Model implementation

Next, we outline how the model components described in Subsections 3.1-3.5 fit together in the overall model. At the highest level, the model constructs a sequence of events (of the seven types described in Subsection 3.1) by scheduling
 430 them, at random, along a master “event timeline”. For each event, the following steps are executed:

1. *Select the agent(s) involved in the event.* This is determined by a variety of factors, e.g. HCWs on scheduled rounds.
2. *For each agent involved in the event, the BPV and IPV are updated to the time (on the event timeline) of the current event.* At the start of the
 435

current event, the BPVs and IPVs of the participating agents reflect the host’s sub-populations at the time of their most-recent previous events.

3. *For an event that involves more than one agent, bacterial exchange between the agents is simulated according to the method in Subsection 3.4.*

440 Figure 1 shows, for an example simulation, a portion of the event timeline. For the interaction event that begins at time t_3 (the current “event time”, as indicated by the clock icon), assume that agents HCW_1 and P_1 have been selected in Step 1 to participate in the event. Prior to executing Step 2 of the event, HCW_1 ’s BPV and IPV contain that agent’s bacteria and immune
445 responder sub-populations, respectively, each evaluated at time t_2 (the time of the most-recent event involving HCW_1). So, in Step 2, HCW_1 ’s BPV and IPV must be updated by applying the in-host model of Subsection 3.3 to advance them from t_2 to the current time t_3 . (See Figure 1.) The BPV and IPV for P_1 are updated in the same way, but from t_1 to t_3 . In Step 3, an opportunity for
450 bacteria transfer, via the method described in Subsection 3.4, between the two agents completes the event.

Our computational model is implemented using MATLAB, allowing us to leverage both the object-oriented programming capabilities of MATLAB for implementing the agent-based portions and differential equations solvers for the
455 intra-host model.

4. Results

To demonstrate the potential of our model as an investigative tool, we present the details of three simulated experiments.

4.1. Hospital-acquired pneumonia

460 We now use our model to simulate the treatment of hospital-acquired pneumonia (HAP) within an intensive care unit. Our goal here is two-fold: To demonstrate how our model may be used to explore HAIs and AR-control measures, while also comparing treatment strategies whose relative strengths are

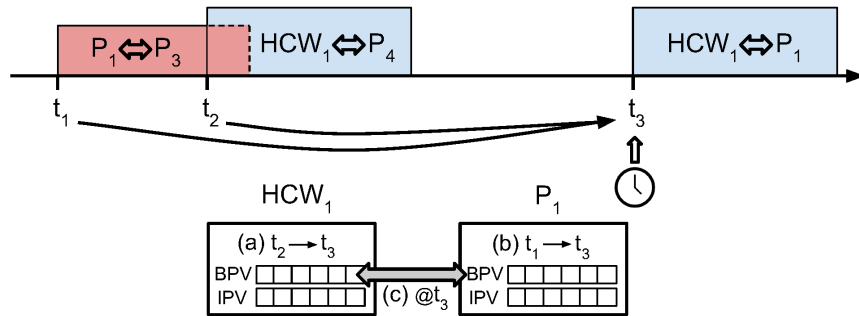


Figure 1: An illustration of part of the example simulation from Section 3.6. The events (shaded boxes) that comprise the simulation occur at randomly-chosen times along the event timeline (horizontal axis). If t_3 represents the start time of the current event, the event unfolds as follows: (a) The BPV and IPV of HCW_1 are updated from t_2 (the time of that agent's most-recent prior event) to the current event time t_3 . (b) The BPV and IPV of P_1 are updated from t_1 (the time of that agent's most-recent prior event) to the current event time t_3 . (c) Two-way bacterial transfer between the two agents.

already generally accepted by practicing clinicians, and are consistent with previous modeling efforts [7]. HAP is the second most common hospital-acquired infection (after urinary tract infections), and a leading cause of HAI-induced mortality [48]. HAP is a particular problem within ICUs, where many patients undergo mechanical ventilation, providing easy accessibility for pathogens to reach the lungs. The two most common pathogens implicated in HAP are *Staphylococcus aureus* and *Pseudomonas aeruginosa*, which together account for nearly 30% of cultured cases [2]. Antibiotic resistant strains of both of these species (including the well-known *methicillin-resistant S. aureus*, or *MRSA*), are widespread, leading to the need for a large arsenal of antibiotics for treating HAP.

Two keys to successful treatment of HAP are (i) early identification of the causative pathogen, and (ii) early determination of the MIC for that pathogen with respect to each of the antibiotics recommended for eliminating them. Together, these ensure that the patient will receive the best choice of antibiotic at a sufficiently high dose, and to avoid attempting to treat them with an ultimately ineffective drug. For this reason, medical researchers have proposed that hospitals screen ICU patients at the first signs of pneumonia [49]. While this

Table 8: The four treatment protocols used in the experiment, in terms of simulation time t , representing the number of hours from initial pneumonia diagnosis. The last four columns indicate the specific antibiotic regimen during different time intervals of the treatment period. Abbreviations in the table: IPM-500 = repeated 500mg. doses of imipenem, OXA-500 = repeated 500mg. doses of oxacillin, OXA-1000 = repeated 1000mg. doses of oxacillin.

Protocol	Time of Pathogen Identification	Time of Completion of MIC-analysis	$0 \leq t \leq 24$	$24 < t \leq 48$	$48 < t \leq 72$	$t > 72$
1	$t = 48$	$t = 72$	IPM-500	IPM-500	OXA-500	OXA-1000
2	$t = 48$	$t = 48$	IPM-500	IPM-500	OXA-1000	OXA-1000
3	$t = 24$	$t = 48$	IPM-500	OXA-500	OXA-1000	OXA-1000
4	$t = 24$	$t = 24$	IPM-500	OXA-1000	OXA-1000	OXA-1000

rationale is widely accepted as sound, in practice many hospitals will culture ICU pneumonia patients only after the first attempt at antibiotic treatment (typically with a broad-spectrum drug) has proven ineffective, reasoning that
495 the procedure for obtaining sputum samples from the lung is not only unpleasant for the patient (For patients unable to produce sputum by coughing, the procedure involves insertion of a sample-gathering device into the lungs.), but also provides an additional opportunity to introduce pathogenic bacteria into the patient’s lower respiratory system.

490 Our experiment will focus specifically on a single patient with HAP caused by infection with a strain of *S. aureus*, and will compare the fate of this patient under each of four treatment protocols, each involving initial treatment with a broad-spectrum antibiotic (imipenem), followed by sputum sample testing to determine the causative pathogen and associated MIC-levels, then a subsequent
495 switch to a narrow-spectrum antibiotic (oxacillin). We will assume that this particular strain of *S. aureus* has a high-level of resistance (i.e. a large MIC-value) with respect to imipenem, and an intermediate-level (i.e. higher than the MIC-levels normally found in samples isolated at this hospital, but low enough to be treatable) of resistance to oxacillin. As illustrated in Table 8,
500 the four protocols differ only in the initiation times for the pathogen identification and MIC-determination procedures (each assumed to be 100% accurate). In Treatments 1 and 2, patients are cultured only if the initial treatment with

Table 9: The four AR-profiles used in the numerical HAP experiment in Sub-Section 4.1.

AR-Profile	MIC vs. Imipenem	MIC vs. Oxacillin
1	0.8	0.4
2	0.8	4.0
3	8.0	0.4
4	8.0	4.0

imipenem (500mg doses, repeated every six hours) is not successful after 24 hours, resulting in a 24-hour lag time in pathogen identification, compared to
505 the immediate culturing of patients undergoing Treatments 3 or 4. Further, Treatments 1 and 3 assume that MIC-analysis requires an additional 24 hours (the current norm), while Treatments 2 and 4 assume that both pathogen identification and MIC-analysis can be completed within a single 24-hour period. Upon pathogen identification (but before MIC-analysis results are available),
510 the imipenem treatment is discontinued, in favor of repeated (every four hours) 500mg doses of oxacillin. After MIC-analysis, the results reveal that the current oxacillin doses are insufficient to raise the patient’s drug-level to exceed the pathogen’s oxacillin-MIC, so the oxacillin dose is then increased to 1000mg.

First, we investigate the effects of early pathogen identification (as in Pro-
515 tocols 3 and 4) by comparing them to the effects of late pathogen identification (as in Protocols 1 and 2). We set up our model with one bacteria species (*S. aureus*), two antibiotics (imipenem and oxacillin), and two resistance levels (low-MIC and high-MIC) for each antibiotic, resulting in the four possible AR-profiles listed in Table 9. The patient’s BPV and IPV will then have the
520 structure shown in the “Bacteria 1” column of Table 4, and we will use the same indexing scheme here. Each entry of the patient’s BPV is set to zero, except for the entry corresponding to C-Cat 4 and AR-profile 3, P_{413} , which is set to 10^5 cells/mL. All entries in the patient’s IPV are also initially set to zero. For this experiment, we do not permit the bacteria to spread to other C-Cats

Table 10: Model parameter values used in the numerical HAP experiment in Sub-Section 4.1.

Parameter	Description (<i>units</i>)	Model Equation	Value	Source
a_{413}	Bacterial growth rate in C-Cat 4 (min^{-1})	(10)	0.0286	[50]
$P_{\text{max},41}$	Bacterial carrying capacity in C-Cat 4 ($P\text{-cells}/\text{mL}$)	(10)	10^{12}	[50]
λ	Immunocompetence parameter (<i>unitless</i>)	(10), (11)	1.0	[46]
b_{41}	Bacterial death rate due to immune response in C-Cat 4 ($P\text{-cells}/(I\text{-cell} \cdot \text{min})$)	(10)	0.0025	[51]
K_{41}	Immune kill rate saturation constant in C-Cat 4 ($P\text{-cells}/\text{mL}$)	(10)	500	estimated
c_{41}	Rate of pathogen-induced immune responder activation in C-Cat 4 ($P\text{-cells}/(\text{mL} \cdot \text{min})$)	(11)	0.001	estimated
B_{41}	Pathogen-induced immune activation saturation constant in C-Cat 4 ($P\text{-cells}/\text{mL}$)	(11)	1000	estimated
d_{41}	Rate of autocatalysis-induced immune responder activation in C-Cat 4 ($I\text{-cells}/(\text{mL} \cdot \text{min})$)	(11)	0.001	estimated
M_{41}	Autocatalysis-induced immune activation saturation constant in C-Cat 4 ($I\text{-cells}/\text{mL}$)	(11)	10.0	estimated
q_{41}	Immune responder decay rate in C-Cat 4 (min^{-1})	(11)	0.0001	[52]
α_{411}	Imipenem-induced kill-rate parameter in C-Cat 4 (min^{-1})	(12)	0.03	estimated
β_{411}	Imipenem-induced kill-rate parameter in C-Cat 4 ($\mu\text{g}/\text{mL}$)	(12)	1.0	estimated
γ_{411}	Imipenem-induced kill-rate parameter in C-Cat 4 (<i>unitless</i>)	(12)	1.0	estimated
α_{412}	Oxacillin-induced kill-rate parameter in C-Cat 4 (min^{-1})	(12)	0.0725	estimated
β_{412}	Oxacillin-induced kill-rate parameter in C-Cat 4 ($\mu\text{g}/\text{mL}$)	(12)	1.0	estimated
γ_{412}	Oxacillin-induced kill-rate parameter in C-Cat 4 (<i>unitless</i>)	(12)	1.0	estimated
Λ_{131}	MIC of pathogen vs. imipenem in R-profile 3 ($\mu\text{g}/\text{mL}$)	(10)	8.0	user-defined
Λ_{132}	MIC of pathogen vs. oxacillin in R-profile 3 ($\mu\text{g}/\text{mL}$)	(10)	4.0	user-defined

525 or to change to another AR-profile via mutation, so the bacteria population is limited to the P_{413} -entry in the patient's BPV for the duration of the experiment. Model parameter values are listed in Table 10, and our results are shown in Figure 2. Figure 2(a) shows the outcomes for our patient under Protocols 2 and 4, the two treatments that assume that both the pathogen identification and the MIC-analysis can be completed within a single 24-hour window, but differ by 24 hours in pathogen identification. Similarly, Figure 2(b) shows the outcomes under Protocols 1 and 3, the two treatments that assume a 24-hour lag time between pathogen identification and MIC determination, but differ by 24 hours in pathogen identification. Each figure shows the patient's *S. aureus* 530 load (in $\log(CFU)$) over the first 72 hours of treatment. In both comparisons, we see that the delay in pathogen identification results in higher pathogen loads. (Note that the changes in slope for each curve correlate to the treatment changes indicated in Table 8.) These results are consistent with the conclusions of [7], where the authors investigate a similar question, using an in-host model that differs from ours. 540

Next, we explore the effects of fast MIC-analysis techniques, by comparing Protocols 2 and 4 (fast MIC-analysis) to Protocols 1 and 3 (24-hour MIC-

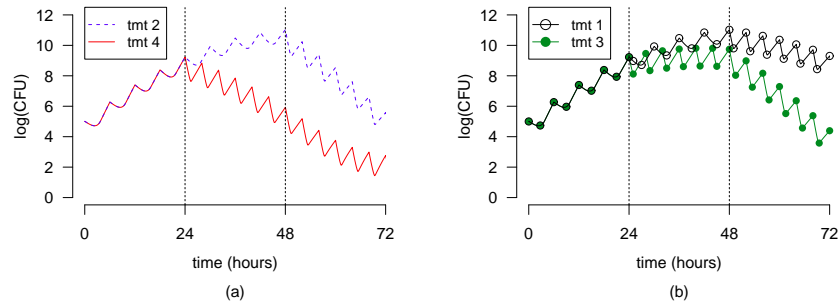


Figure 2: (a) Pathogen load ($\log(CFU)$) versus time (hours) for a HAP patient under treatment Protocols 2 (dashed) and 4 (solid) for the first 72 hours after the initiation of treatment. The pathogen load increases during the period of imipenem treatment (0–48 hours under Protocol 2 and 0–24 hours under Protocol 4). In each case, after identification of the pathogen (at 48 hours under Protocol 2 and at 24 hours under Protocol 4), the pathogen load then decreases in response to the corresponding switch to the larger dose of oxacillin. (b) Pathogen load versus time for a HAP patient under treatment Protocols 1 (open circles) and 3 (filled circles) for the first 72 hours after the initiation of treatment. In each case, after identification of the pathogen (at 48 hours under Protocol 1 and at 24 hours under Protocol 3), the pathogen load then continues to increase, albeit at a reduced rate, during the period of insufficient dosage of oxacillin (48–72 hours under Protocol 1 and 24–48 hours under Protocol 3).

analysis). Our results are shown in Figure 3, which exhibits the pathogen load, beginning at the initial switch from imipenem to oxacillin, for each of the four
545 treatment protocols. Figure 3(a) shows the outcomes for the patient under Protocols 3 and 4, the two treatments that switch from imipenem to oxacillin after 24 hours, but differ by 24 hours in MIC-analysis. Similarly, Figure 3(b) shows the outcomes under Protocols 1 and 2, the two treatments that switch from imipenem to oxacillin after 48 hours, but differ by 24 hours in MIC-analysis.
550 In both comparisons, we see that the delay in MIC-analysis results in higher pathogen loads. In Figure 4, we display the patient’s pathogen loads under all four treatment protocols, to permit further comparison. It is significant to note the differences in the maximum pathogen loads between protocols (some of which may well reach fatal levels during the treatment process), due to the delays
555 in pathogen identification (in Protocols 1 and 2) and in MIC determination (in Protocols 1 and 3). Quantification of these differences in this way will likely prove useful in further comparisons of the four treatment strategies.

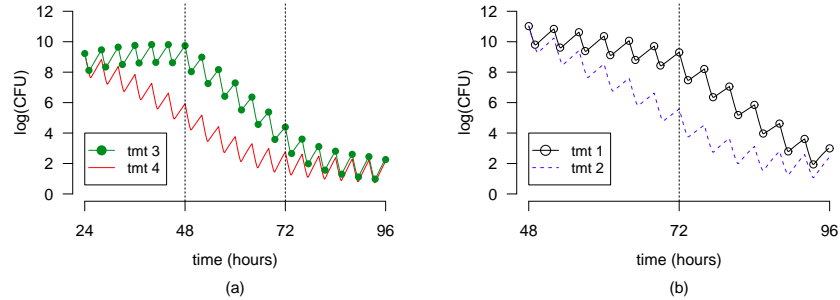


Figure 3: (a) Pathogen load ($\log(CFU)$) versus time (hours) for a HAP patient under treatment Protocols 3 (filled circles) and 4 (solid) for the period of 24–96 hours after the initiation of treatment. In each case, pathogen identification, and the resulting switch to oxacillin, occur at 24 hours. Under Protocol 3, the pathogen load increases during the period of insufficient dosage of oxacillin (24–48 hours). However, in each case, after MIC determination (at 48 hours under Protocol 3 and at 24 hours under Protocol 4), the pathogen then load decreases in response to the switch to the larger dose of oxacillin. (b) Pathogen load versus time for a HAP patient under treatment Protocols 1 (open circles) and 2 (dashed) for the period of 48–96 hours after the initiation of treatment. In each case, pathogen identification occurs at 48 hours. Under Protocol 1, the pathogen load increases during the period of insufficient dosage of oxacillin (48–72 hours), but in each case, after MIC determination (at 72 hours under Protocol 1 and at 48 hours under Protocol 2), the pathogen load decreases in response to the switch to the larger dose of oxacillin.

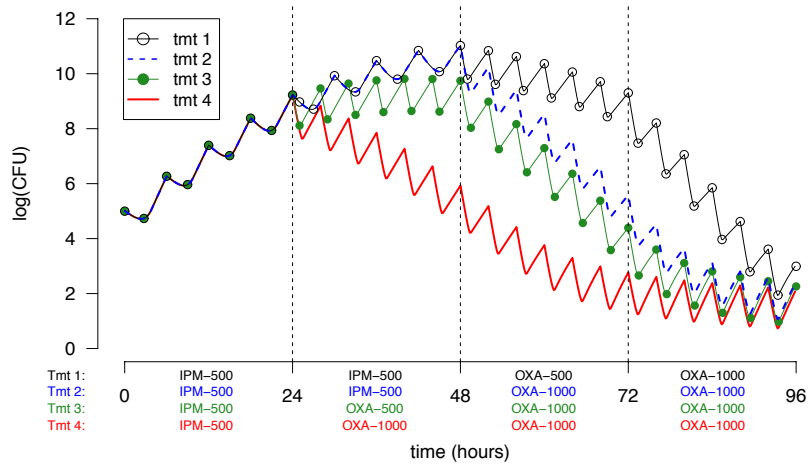


Figure 4: Pathogen load ($\log(CFU)$) versus time (hours) for a HAP patient under treatment Protocols 1 (open circles), 2 (dashed), 3 (filled circles), and 4 (solid) for the first 96 hours after the initiation of treatment. Note the differences in the maximum pathogen load for each protocol, due to differences in the timing of pathogen identification and MIC-analysis.

4.2. Infection spread with multiple patients

The next demonstrations illustrate the ability of the agent-based portion
560 of our model to realistically reflect heterogeneity among individuals. Here, we
model one HCW visiting two different patients on rounds. The time required to
administer care to a patient on each HCW visit is drawn from a Gamma(40,0.25)
distribution with mean 10 minutes and standard deviation 1.58 minutes, with
visits alternating between the two patients, with no downtime between consecu-
565 tive visits. Each visit provides an opportunity to transfer bacteria between the
patient and HCW, consistent with the possible exchanges presented in Table 6.
(For this demonstration, we do not permit bacterial exchange directly between
the two patients.) Bacteria transfer proceeds as described in Section 3.4. We
present results both in the case of a low transfer probability (equal to 0.01) and
570 in the case of a high transfer probability (equal to 0.1). For each interaction in
which transfer is to occur, we fix the fraction of transferred bacteria to be 0.02.
Hence, the results to follow feature two sources of randomness: the service time
for each patient visit, and the per-visit determination of whether bacteria are
transferred between the HCW and patient.

575 For these demonstrations, we include two pathogen species and one AR-
profile, so each agent's BPV has exactly 12 entries. For the first demonstration,
each agent (HCW and both patients) has a zero for each BPV-entry, with the
following exceptions:

- Patient 1 has 10^5 bacteria/mL of pathogen 1 in C-Cat 1.
- 580 • Patient 2 has 10^5 bacteria/mL of pathogen 2 in C-Cat 1.

Figure 5 depicts the pathogen loads in each of the six C-Cats for the HCW
and the two patients, both initially and after eight hours. As shown in Fig-
ure 5(a)–(c), the HCW starts initially with no pathogens in any C-Cat. Patient
1 and Patient 2 each have a different pathogen, but same initial loads, present in
585 C-Cat 1 only. Figure 5(d)–(f) depicts the mean pathogen loads after eight hours
(starting from the initial loads) under low probability (Bernoulli with $p = 0.01$)

of bacterial transfer. Under this low probability, we replicated the simulation 360 times, and, for each C-Cat, considered only the non-zero values present in that C-Cat across the replications. This collection of non-zero values was used
590 to compute the mean, and a 90% tolerance interval, for the pathogen load in that C-Cat. (A bar plot beneath each of Figures 5(d)-(f) indicates, for each C-Cat entry, the percentage out of the 360 replications in which the C-Cat entry resulted in a non-zero value.)

Figure 5(g)-(i) depicts the mean pathogen loads after eight hours (again
595 starting from the initial loads) under high probability of bacterial transfer (Bernoulli with $p = 0.1$). Again, we replicated the simulation 360 times. For each C-Cat, we selected at random (from among all the 360 replications) the same number of values as were used to compute the mean and tolerance interval in the low-probability setting. Although the majority of replications here
600 resulted in non-zero values present in each C-Cat, using the same number of (randomly chosen) values here allows us to present tolerance intervals that are consistent in both the low- and high-probability settings.

Next, we demonstrate that individual variations can result, even when our model is applied to hosts that are initially identical. Here, Patient 1 and Patient
605 2 will begin with identical initial pathogen loads – 10^5 bacteria/mL of pathogen 1 in C-Cat 1 and 10^5 bacteria/mL of pathogen 2 in C-Cat 2. The HCW will begin with a BPV equal to the zero vector. Figure 6 depicts the pathogen loads in each of the six C-Cats for the HCW and the two patients, both initially and after eight hours. Mean pathogen loads and corresponding 90% tolerance
610 intervals were computed similar to that for Figure 5, but using 240 replications. (Because of the larger initial bacterial loads, fewer replications were required to achieve sufficient non-zero values to produce 90% tolerance intervals.) Again, notice that bacteria of both types are now present in various C-Cats for the HCW and both patients, and that the C-Cats populated are fully consistent
615 with the possible transfers presented in Table 6. Moreover, for both the low and high probability simulations, Patient 1 and Patient 2, who had identical loads initially, have, after eight hours, pathogen loads that differ from each

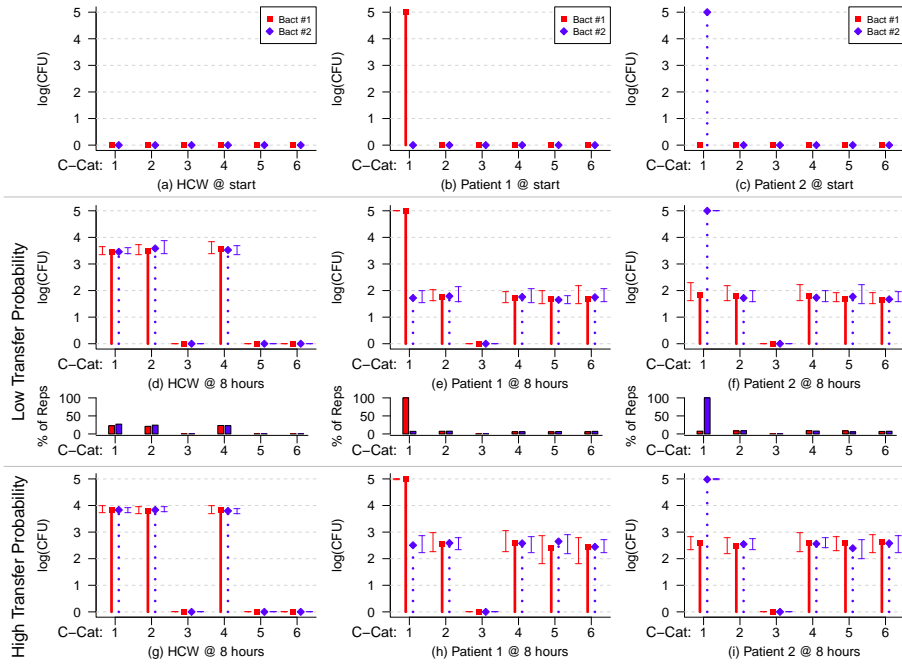


Figure 5: Pathogen load ($\log(CFU)/mL$) for two different bacteria species (indicated by squares and diamonds, respectively) in each of the six colonization categories at different points in time for one HCW visiting two different patients on rounds. Each given value represents the mean of non-zero values from among 360 replications. Next to each is a vertical bar to indicate a 90% tolerance interval. (a)–(c) Initial pathogen loads of two different bacteria species for the HCW, Patient 1, and Patient 2. (d)–(f) Resulting pathogen loads after eight hours under low probability (Bernoulli with $p = 0.01$) of pathogen transfer, and histograms indicating the percentage of replicates that yielded non-zero bacterial loads in each C-Cat. (g)–(i) Resulting pathogen loads after eight hours under high probability (Bernoulli with $p = 0.1$) of pathogen transfer. Note that, although Patient 1 initially carries only the first bacteria species and Patient 2 only the second, patient-to-HCW and HCW-to-patient transfer across time result in both bacteria species being spread, in different amounts, among the HCW and both patients.

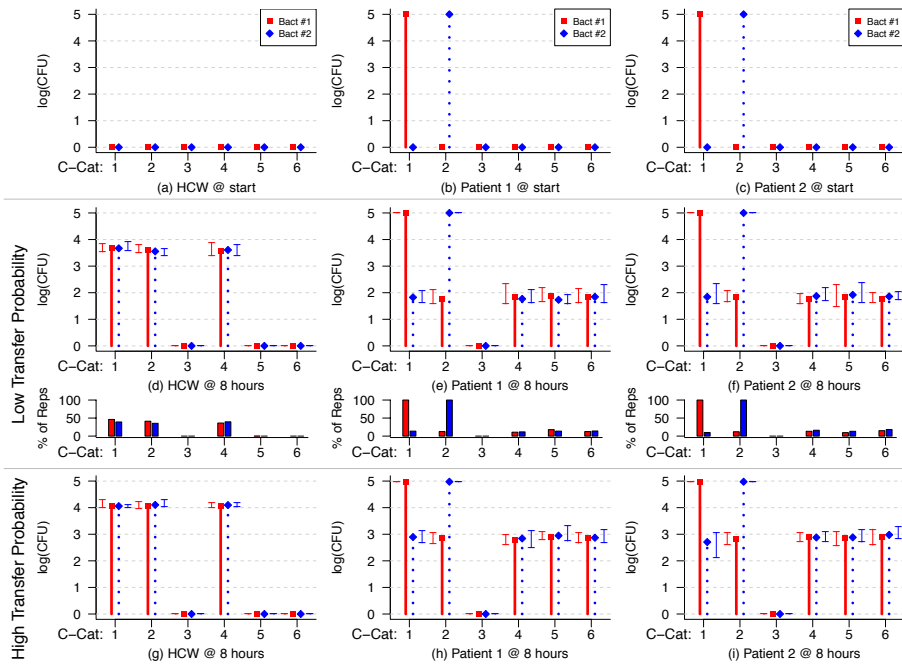


Figure 6: Pathogen load ($\log(CFU/mL)$) for two different bacteria species (indicated by squares and diamonds, respectively) in each of the six colonization categories at different points in time for one HCW visiting two different patients on rounds. Each given value represents the mean of non-zero values from among 240 replications. Next to each is a vertical bar to indicate a 90% tolerance interval. (a)–(c) Initial pathogen loads of two different bacteria species for the HCW, Patient 1, and Patient 2. (d)–(f) Resulting pathogen loads after eight hours under low probability (Bernoulli with $p = 0.01$) of pathogen transfer, and histograms indicating the percentage of replicates that yielded non-zero bacterial loads in each C-Cat. (g)–(i) Resulting pathogen loads after eight hours under high probability (Bernoulli with $p = 0.1$) of pathogen transfer. Note that, although both patients start with identical pathogen loads of both bacteria species, transfer across time results in a heterogeneous distribution of pathogen loads for the otherwise identical patients.

other. This demonstrates the capacity for heterogeneity of individuals across time, distinguishing our agent-based approach from a strictly compartmental model.

4.3. Effects of service times on infection spread

Our final example illustrates how our model may be used to investigate clinically-relevant questions through simulation of controlled experiments, even in the presence of heterogeneities in patient status, event types, and mean-times between events. Here, we include one bacteria species (*S. aureus*), one antibiotic

(imipenem), and two MIC-levels, resulting in two bacterial strains (one for each MIC-level), which, for convenience, we will call “sensitive” and “resistant”. We include four patients (labeled P1, P2, P3, P4) and one HCW. At the start of the simulation, the HCW is bacteria-free, while each patient carries 10^4 CFU/ml of bacteria in its C-Cat 5; P4 carries the resistant strain, while the other three carry the sensitive strain. We assume that each patient, due to differing comorbidities, requires a different level-of-care, reflected in the length of time (i.e. service time) that the HCW spends with each. The HCW visits one patient at the start of each hour, and rotates between them, so each patient is visited every four hours. The duration of each visit is drawn from a Gamma distribution with standard deviation 1.58 minutes and a mean of 5 minutes for P1, 10 minutes for P2, and 15 minutes for P3. We are interested in the influence that P4’s service time has on the spread of the resistant strain (initially carried by P4 only) of *S. aureus* over a 72-hour period. We investigate this by varying P4’s service time and observing the resulting prevalence of the resistant bacteria in the other three patients.

In this experiment, bacteria can mutate from one MIC-level to the other, with a mutation probability of 10^{-5} . Transfers of bacteria between interacting agents are possible, according to Table 6, with probability of transfer during an interaction of length Δ minutes computed according to formula (7), with $\alpha = 0.05$. For each transfer from a BPV-entry of one agent (the donor), 2% of the bacteria from that BPV-entry is transferred to the receiving agent.

Each patient visit is comprised of two steps, with a conditional third step:

1. At the start time of the visit, the HCW’s bacteria load in C-Cat 1 is reduced by 90%, reflecting effective handwashing and sterilization of equipment.
2. Possible pathogen exchange.
3. (*Conditional*) The patient is given a 500 mg. dose of imipenem.

The conditional third step is based on our one included antibiotic-treatment protocol: A course of six doses, given four hours apart, each dose consisting of

500mg of imipenem, administered as IV bolus. We assume that each patient will begin to exhibit symptoms of infection when that patient's pathogen load exceeds 10^4 in any C-Cat. Consequently, a new course of antibiotics will be prescribed during a patient visit, provided this threshold condition is exceeded, unless the patient is already receiving antibiotic treatment, in which case Step 3 is also executed. This treatment protocol results in serum imipenem concentrations that exceed the MIC for the sensitive strain, but not the resistant strain.

We use the parameter values from Table 10 (with the subscripts suitably changed for the present setting), with the following exceptions:

- Here, we use $P_{max,i1} = 10^8$ for each C-Cat i .
- The oxacillin parameters listed in Table 10 do not apply here.
- The MIC-values for imipenem are now $\Lambda_{111} = 0.8$ and $\Lambda_{121} = 8.0$ for the sensitive and resistant strains, respectively.

We run a total of 60 replications of the following experiment:

- Conduct the one HCW-four-patient simulation for a 72-hour period, repeated 40 times.
- Count the number of these 40 runs for which patient P1 has a non-zero population of the resistant pathogen strain after 36 hours and after 72 hours.
- Repeat the previous bullet for patient P2 and for patient P3.
- Use the data gathered to compute the frequency of resistant pathogen carriage in each of P1, P2, and P3 at 36 hours and at 72 hours.

After completion of the 60 replications (requiring about five hours of computing time on across 40 nodes (10 quad-core Intel Core i5-4570 CPUs @ 3.20GHz, running Red Hat Enterprise Linux Workstation release 7.2 (Maipo)), we compute the mean of each of the six quantities computed from each replication,

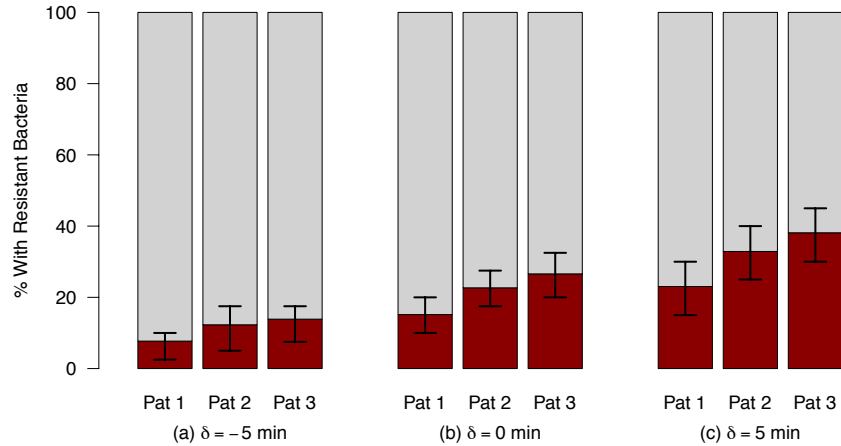


Figure 7: The prevalence (as percentage of 60 replications) of resistant *S. aureus* infection in at least one C-Cat of Patients P1, P2, and P3, after 36 hours, when Patient P4’s mean service time is $10 + \delta$ minutes. Results are for (a) $\delta = -5$, (b) $\delta = 0$, and (c) $\delta = 5$. In each case, vertical bars indicate 95% tolerance intervals.

along with a 90% tolerance interval for each. This experiment is conducted for three different service times for patient P4: 5, 10, and 15 minutes. Results are
 685 shown in Figures 7 and 8.

As expected, prevalence increases with larger mean service times, with differences in prevalence between the three patients reflective of their differing service times. More noteworthy, results like this can be refined (e.g. by including a finer mesh of time-values and δ -values) to derive an approximate functional form for the dependence of prevalence on these parameters. Quantitative results like
 690 this, reflecting several levels of heterogeneity, can provide added precision and specificity to the design of resistance-control measures.

5. Discussion

We have presented a new model for simulating the spread of antibiotic-resistant infections in hospital wards. This model links an agent-based structure
 695 at the patient/HCW interaction level with a very detailed differential equations and probabilistic model at the in-host level. We have demonstrated the potential

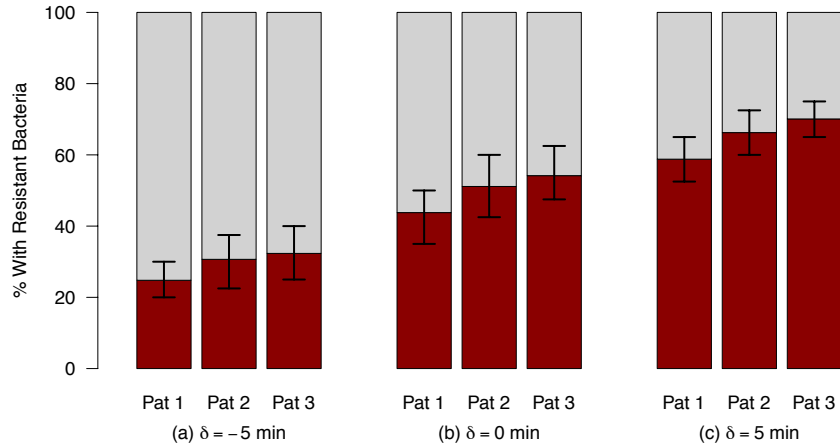


Figure 8: The prevalence (as percentage of 60 replications) of resistant *S. aureus* infection in at least one C-Cat of Patients P1, P2, and P3, after 72 hours, when Patient P4’s mean service time is $10 + \delta$ minutes. Results are for (a) $\delta = -5$, (b) $\delta = 0$, and (c) $\delta = 5$. In each case, vertical bars indicate 90% tolerance intervals.

usefulness of this model by investigating four different treatment strategies for pneumonia caused by *S. aureus*. We have also demonstrated the strength of
700 agent-based simulation in this context – simulating interactions, each with the potential for bacterial transfer, between individuals having heterogeneous and dynamic characteristics. We concluded by demonstrating the potential of our model to incorporate several levels of heterogeneity, both in terms of patient characteristics, and in ward-level dynamics. In future work, we will present
705 further experiments, that will fully encompass both the inter-host and in-host components of our model.

The present work has the potential to serve multiple purposes with regard to antibiotic resistance and hospital-acquired infections. As noted in Section 1, we designed our model as a tool to permit researchers and health-care profession-
710 als opportunities to simulate control strategies to assess their relative merits, without risking real patients. In addition, this model, and resulting simulation tool, may serve a valuable educational role, providing opportunities to train health-care workers on the consequences of infection-control decisions.

In our effort to create a realistic model that covers multiple levels of dynam-
715 ics, we face the challenge of deriving reliable estimates for many model param-
eters. Many have direct biophysical interpretations, and can be estimated from
experimental data (provided the data exists), while others arise from mathe-
matical constructs (e.g. saturation constants), and can be estimated from data
720 only indirectly, through calibration procedures. These efforts are ongoing with
the authors, and are likely to lead to ideas for new laboratory experimentation.
Our next order of business will be a thorough sensitivity analysis to identify
those parameters which have the greatest impact on model outcomes. This will
require two very different approaches, given the significant roles that both dif-
ferential equations and agent-based models play in the overall infection model.
725 Results will be reported in a future paper.

In other future work, we will extend this model to incorporate additional
factors including:

- *Agent self-interaction events*: It is often the case that a bacteria species
can be harmless in some agent C-Cats but pathogenic in other C-Cats. It
730 is possible, e.g., through inadequate personal hygiene, to induce infection
in oneself by transferring such bacteria from a “safe” C-Cat to a less-
safe one. We will extend the model to include an event type for agents
interacting with themselves, to permit the transfer of bacteria between
C-Cats of a single agent.
- *Indicators of infection severity*: Our model currently uses bacteria counts
735 to measure infection severity. In practice, these numbers are seldom
known, and clinicians rely on indirect measures of infection severity, such
as body temperature, white blood cell count, and other morbidities. We
will investigate the relationship between these quantities and bacterial load
740 to incorporate these indirect signs, thereby permitting us to more-closely
parallel the usual patterns of antibiotic therapy.
- *Agent mortality*: Currently there is no mechanism whereby an agent can
die from infection, regardless of how large the pathogen load becomes. We

will incorporate a mechanism whereby mortality will become possible for
745 agents with very high bacterial loads in the most sensitive C-Cats.

- *Refined handling of AR-profiles:* We will extend the current means of modeling antibiotic resistance profiles to permit the number of MIC-values (the parameter N in equations (1)-(2) to differ between different bacteria-antibiotic pairs. The current model will also be expanded to allow for
750 the phenomenon of cross-resistance, in which the mechanism (e.g. efflux pumps in *Pseudomonas aeruginosa* [53]) by which a bacterium achieves resistance to one antibiotic may afford resistance to certain other antibiotics as well.
- *Bacterial toxins:* A number of important hospital pathogens, including *S. aureus* and *P. aeruginosa*, produce toxins that can influence the severity
755 of an HAI, and which can remain in the body even after the pathogen population has been cleared. We will incorporate the dynamics of these toxins into the existing in-host model.
- *Antibiotic toxicity:* Any antibiotic, in sufficiently-high concentrations, will
760 be toxic to humans. We will incorporate the effects of antibiotic toxicity into our model to more accurately reflect the limitations faced by prescribing medical personnel.
- *Antibiotic interactions:* The present model permits treatment of a host with two or more antibiotics simultaneously, and assumes that the bacteriocidal effects are independent and additive. Clinical evidence suggests
765 that there are certain antibiotic combinations for which this assumption is not valid ([54, 55]). We will adapt our model to allow for the possibility of both synergistic and antagonistic effects of antibiotic combination therapies.
- *The role of indwelling devices:* It is widely accepted that the use of certain indwelling devices (e.g. mechanical ventilators, artificial heart valves,
770 urinary and central venous catheters) significantly increases a patient's

risk for developing an HAI [56], and may influence the risk of antibiotic resistance [57]. We will extend the model to simulate the connections between HAIs and these devices, to accurately incorporate these important dynamics.

- *The role of fomites in HAI*: Researchers acknowledge a potential role for environmental surfaces (fomites) to serve as avenues for pathogen transfer ([58, 59]). We will expand our model to include the effects of fomite transfer of pathogens, with the goal of simulating experiments to determine the impact on resistance-levels of a number of proposed disinfection measures ([60, 61]).

We are currently developing a graphical user interface to facilitate model use, and, upon completion, will make our MATLAB implementation publicly available.

Acknowledgements

The authors are grateful to the University of Richmond for providing summer research support, to Andreea Iovan for her work on a graphical interface for the model, and to the reviewers, whose valuable input led to a much-improved version of this paper.

References

- [1] Office of Disease Prevention and Health Promotion, National action plan to prevent health care-associated infections: Road map to elimination, http://www.health.gov/hcq/prevent_hai.asp, accessed May 12, 2015 (2015).
- [2] S. Magill, J. Edwards, W. Bamberg, Z. Beldavs, G. Dumyati, M. Kainer, R. Lynfield, M. Maloney, L. McAllister-Hollod, J. Nadle, S. Ray, D. Thompson, L. Wilson, S. Fridkin, Multistate point-prevalence survey of health care-associated infections, *N. Engl. J. Med.* 370 (2014) 1198–1208.

- [3] Centers for Disease Control and Prevention, Antibiotic/Antimicrobial Resistance, <http://www.cdc.gov/drugresistance/>, accessed May 12, 2015 (2015).
800
- [4] A. Fleming, Penicillin, in: Nobel Lectures: Physiology or Medicine (1942-1962), World Scientific, Singapore, 1999, pp. 83–93.
- [5] S. Levy, The challenge of antibiotic resistance, *Sci. Amer.* 278 (1998) 46–53.
- [6] R. Moellering, H. Blumgart, Understanding antibiotic resistance development in the immunocompromised host, *Int.l J. Infect. Dis.* 6 (2002) S3–S4.
805
- [7] E. D’Agata, M. Dupont-Rouzeyrol, P. Magal, D. Olivier, S. Ruan, The impact of different antibiotic regimens on the emergence of antimicrobial-resistant bacteria, *PLoS ONE* 3 (12) (2008) e4036. doi:10.1371/journal.pone.0004036.
810
- [8] T. Felton, J. Goodwin, L. OConnor, A. Sharp, L. Gregson, J. Livermore, S. Howard, M. Neely, W. Hope, Impact of bolus dosing versus continuous infusion of piperacillin and tazobactam on the development of antimicrobial resistance in *Pseudomonas aeruginosa*, *Antimicrob. Agents Chemother.* 57 (12) (2013) 5811–5819.
815
- [9] A. Garber, Antibiotic exposure and resistance in mixed bacterial populations, *Theor. Pop. Biol.* 32 (1987) 326–346.
- [10] P. Geli, R. Laxminarayan, M. Dunne, D. Smith, “One-size-fits-all? Optimizing treatment duration for bacterial infections, *PLoS ONE* 7 (1). doi:10.1371/journal.pone.0029838.
820
- [11] M. Lipsitch, B. Levin, The population dynamics of antimicrobial chemotherapy, *Antimicrob. Agents Chemother.* 41 (1997) 363–373.
- [12] M. Lipsitch, B. Levin, Population dynamics of tuberculosis treatment: Mathematical models of the roles of non-compliance and bacterial heterogeneity in the evolution of drug resistance, *Int. J. Tuberc. Lung Dis.* 2 (1998) 187–199.
825

- [13] L. Terner, R. Dyson, A.-M. Krachler, S. Jabbari, Bacterial fitness shapes the population dynamics of antibiotic-resistant and susceptible bacteria in a model of combined antibiotic and anti-virulence treatment, *J. Theor. Biol.* 372 (2015) 1–11.
- 830
- [14] C. Bergstrom, M. Lo, M. Lipsitch, Ecological theory suggests that antimicrobial cycling will not reduce antimicrobial resistance in hospitals, *Proc. Natl. Acad. Sci. USA* 101 (2004) 13285–13290.
- [15] B. Cooper, G. Medley, S. Stone, C. Kibbler, B. Cookson, J. Roberts, G. Duckworth, R. Lai, S. Ebrahim, Methicillin-resistant *Staphylococcus aureus* in hospitals and the community: Stealth dynamics and control catastrophes, *Proc. Natl. Acad. Sci. USA* 101 (2004) 10233–10238.
- 835
- [16] E. Armeanu, M. Bonten, Control of vancomycin-resistant *enterococci*: One size fits all?, *Clin. Infect. Dis.* 41 (2005) 210–216.
- [17] E. D’Agata, G. Webb, M. Horn, A mathematical model quantifying the impact of antibiotic exposure and other interventions on the endemic prevalence of vancomycin-resistant *enterococci*, *J. Infect. Dis.* 192 (2005) 2004–2011.
- 840
- [18] M. Haber, B. Levin, P. Kramarz, Antibiotic control of antibiotic resistance in hospitals: A simulation study, *BMC Infect. Dis.* 10 (2010) 254–263.
- 845
- [19] T. Doan, D. Kong, C. Marshall, C. Kirkpatrick, E. McBryde, Modeling the impact of interventions against *Acinetobacter baumannii* transmission in intensive care units, *Virulence* 7 (2) (2016) 141–152.
- [20] V. Sypsa, M. Psychogiou, G.-A. Bouzala, L. Hadjihannas, A. Hatzakis, Transmission dynamics of carbapenemase-producing *Klebsiella pneumoniae* and anticipated impact of infection control strategies in a surgical unit, *PLoS ONE* 7 (7) (2012) e41068. doi:10.1371/journal.pone.0041068.
- 850
- [21] R. Anderson, R. May, *Infectious Diseases of Humans: Dynamics and Control*, Oxford University Press, Oxford, 1991.

- 855 [22] F. Chamchod, S. Ruan, Modeling the spread of methicillin-resistant *Staphylococcus aureus* in nursing homes for elderly, PLOS One 7 (1) (2012b) e29757.
- [23] I. Pelupessy, M. Bonten, O. Diekmann, How to assess the relative importance of different colonization routes of pathogens within hospital settings, Proc. Natl. Acad. Sci. USA 99 (2002) 5601–5605.
- 860 [24] C. Schultsz, M. Bootsma, H. Loan, T. Nga, L. Thao, T. Thuy, J. Campbell, L. Vien, N. Hoa, N. Hoang, F. Wit, N. Chau, J. Farrar, M. Bonten, L. Yen, Effects of infection control measures on acquisition of five antimicrobial drug-resistant microorganisms in a tetanus intensive care unit in Vietnam, Intensive Care Med. 39 (2013) 661–671.
- 865 [25] V. Seville, S. Chevret, A.-J. Valleron, Modeling the spread of resistant nosocomial pathogens in an intensive-care unit, Infect. Control Hosp. Epidemiol. 18 (1997) 84–92.
- [26] E. D’Agata, M. Horn, S. Ruan, G. Webb, J. Wares, Efficacy of infection control interventions in reducing the spread of multidrug-resistant organisms in the hospital setting, PLoS ONE 7 (2) (2012) e30170. doi: 10.1371/journal.pone.0030170.
- 870 [27] J. Wang, L. Wang, P. Magal, Y. Wang, J. Zhuo, X. Lu, S. Ruan, Modelling the transmission dynamics of methicillin-resistant *Staphylococcus aureus* in Beijing Tongren hospital, J. Hosp. Infect. 79 (2011) 302–308.
- 875 [28] L. Temime, Y. Pannet, L. Kardas, L. Opatowski, D. Guillemot, P. Boelle, Nososim: An agent-based model of pathogen circulation in a hospital ward, in: G. Wainer, C. Shaffer, R. McGraw, M. Chinni (Eds.), Proceedings of the 2009 Spring Simulation Multiconference, Society for Computer Simulation International, San Diego, 2009.
- 880 [29] S. Barnes, B. Golden, E. Wasil, MRSA transmission reduction using agent-

- based modeling and simulation, *INFORMS J. Comput.* 22 (4) (2010) 635–646.
- [30] Y. Meng, R. Davies, K. Hardy, P. Hawkey, An application of agent-based simulation to the management of hospital-acquired infection, *J. Simulation* 4 (2010) 60–67.
- [31] S. Deeny, C. Worby, O. Auguet, B. Cooper, J. Edgeworth, B. Cookson, J. Rotherham, Impact of muprocain resistance on the transmission and control of healthcare-associated MRSA, *J. Antimicrob. Chemother.* 70 (12) (2015) 3366–3378.
- [32] L. Kardaś-Słoma, P.-Y. Boëlle, L. Opatowski, D. Guillemot, L. Temime, Antibiotic reduction campaigns do not necessarily decrease bacterial resistance: the example of methicillin-resistant *Staphylococcus aureus*, *Antimicrob. Agents Chemother.* 57 (9) (2013) 4410–4416.
- [33] C. Macal, M. North, N. Collier, V. Dukic, D. Lauderdale, M. David, R. Daum, P. Shumm, R. Daum, J. Evans, J. Wilder, D. Wegener, Modeling the spread of community-associated MRSA, in: C. Laroque, J. Himmelspach, R. Pasupathy, O. Rose, A. Uhrmacher (Eds.), *Proceedings of the 2012 Winter Simulation Conference, IEEE, Berlin, 2012*.
- [34] M. Boni and M. Feldman, Evolution of Antibiotic Resistance by Human and Bacterial Niche Construction, *Evolution* 59 (2005) 477–491.
- [35] L. Temime and P.-Y. Boëlle and P. Courvalin and D. Guillemot, Bacterial Resistance to Penicillin G by Decreased Affinity of Penicillin-Binding Proteins: A Mathematical Model, *Emerg. Infect. Dis.* 9 (2003) 411–417.
- [36] L. Opatowski and J. Mandel and E. Varon and P.-Y. Boëlle and L. Temime and D. Guillemot, Antibiotic Dose Impact on Resistance Selection in the Community: a Mathematical Model of β -Lactams and *streptococcus pneumoniae* Dynamics, *J. Antimicrob. Chemother.* 54 (2010) 2330–2337.

- [37] F. Stewart and R. Antia and B. Levin and M. Lipsitch and J. Mittler,
910 The Population Genetics of Antibiotic Resistance II: Analytic Theory for
Sustained Populations of Bacteria in a Community of Hosts, *Theor. Pop.*
Biol. 53 (1998) 152–165.
- [38] G. Webb, E. D’Agata, P. Magal, S. Ruan, A model of antibiotic-resistant
bacterial epidemics in hospitals, *Proc. Natl. Acad. Sci. USA* 102 (2005)
915 13343–13348.
- [39] E. D’Agata, P. Magal, S. Ruan, G. Webb, Asymptotic behavior in nosoco-
mial epidemic models with antibiotic resistance, *Diff. Int. Eqns.* 19 (2006)
573–600.
- [40] S. Barnes, A. Harris, B. Golden, E. Wasil, J. Furuno, Contribution of
920 interfacility patient movement to overall methicillin-resistant *Staphylococ-*
cus aureus prevalence levels, *Infection Control and Hospital Epidemiology*
32 (11) (2011) 1073–1078.
- [41] A. Djanatliev, R. German, P. Kolominsky-Rabas, B. Hofmann, Hybrid
simulation with loosely coupled system dynamics and agent-based models
925 for prospective health technology assessments, in: C. Laroque, J. Him-
melspach, R. Pasupathy, O. Rose, A. Uhrmacher (Eds.), *Proceedings of*
the 2012 Winter Simulation Conference, IEEE, Berlin, 2012.
- [42] H. Rahmandad, J. Sterman, Heterogeneity and network structure in the
dynamics of diffusion: Comparing agent-based and differential equation
930 models, *Mgt. Sci.* 54 (5) (2008) 998–1014.
- [43] D. Helbing, S. Balietti, How to do agent-based simulations in the future:
From modeling social mechanisms to emergent phenomena and interactive
systems design, Tech. Rep. 2011-06-024, Santa Fe Institute, Santa Fe, New
Mexico, available via [http://www.santafe.edu/media/workingpapers/](http://www.santafe.edu/media/workingpapers/11-06-024.pdf)
935 [11-06-024.pdf](http://www.santafe.edu/media/workingpapers/11-06-024.pdf) [accessed 1 July 2013]. (2011).

- [44] L. M. Leemis, S. K. Park, Discrete-Event Simulation: A First Course, Pearson Prentice Hall, Upper Saddle River, New Jersey, 2006.
- [45] L. Caudill, B. Lawson, A hybrid agent-based and differential equations model for simulating antibiotic resistance in a hospital ward, in: R. Pasupathy, S.-H. Kim, A. Tolk, R. Hill, M. Kuhl (Eds.), Proceedings of the 2013 Winter Simulation Conference, IEEE, Piscataway, NJ, 2013, pp. 1419–1430.
- [46] L. Caudill, A single-parameter model of the immune response to bacterial invasion, Bull. Math. Biol. 75 (2013) 1434–1449.
- [47] J. Gabrielsson, D. Weiner, Pharmacokinetic and Pharmacodynamic Data Analysis 3e, Swedish Pharmaceutical Society, Stockholm, Sweden, 2000.
- [48] A. Torres, Antibiotic treatment against methicillin-resistant *Staphylococcus aureus* hospital- and ventilator-acquired pneumonia: A step forward but the battle continues, Clinical Infectious Diseases 54 (2012) 630–632.
- [49] B. Spellberg, R. Guidos, D. Gilbert, J. Bradley, H. Boucher, W. Scheld, J. Bartlett, J. Edwards, The epidemic of antibiotic-resistant infections: A call to action for the medical community from the infectious diseases society of america, Clinical Infectious Diseases 46 (2008) 155–164.
- [50] G. Kaatz and S. Seo and N. Dorman and S. Lerner, Emergence of Teicoplanin Resistance during Therapy of *Staphylococcus aureus* Endocarditis, J. Infect. Dis. 162 (1990) 103–108.
- [51] A. Brandwood and K. Noble and K. Schindhelm, Phagocytosis of carbon particles by macrophages in vitro, Biomaterials 13 (9) (1992) 646–648.
- [52] A. Reynolds and J. Rubin and G. Clermont and J. Day and Y. Vodovotz and G. Ermentrout, A Reduced Mathematical Model of the Acute Inflammatory Response: I. Derivation of Model and Analysis of Anti-Inflammation, J. Theor. Biol. 242 (1) (2006) 220–236.

- [53] R. Chuanchuen and K. Beinlich and T. Hoang and A. Becher and R. Karkhoff-Schweizer and H. Schweizer, Cross-resistance between triclosan and antibiotics in *pseudomonas aeruginosa* is mediated by multidrug efflux pumps: exposure of a susceptible mutant strain to Triclosan selects *nfxB* mutants overexpressing MexCD-OprJ, *J. Antimicrob. Chemother.* 45 (2001) 428–432.
- 965
- [54] J. Schentag and L. Strenkoski-Nix and D. Nix and A. Forrest, Pharmacodynamic interactions of antibiotics alone and in combination, *Clin. Infect. Dis.* 27 (1998) 40–46.
- 970
- [55] V. Lázár and I. Nagy and R. Spohn and B. Csörgö and Á. Györkei and Á. Nyerges and B. Horváth and A. Vörös and R. Busa-fekete and M. Hrtyan and B. Bogos and O. Méhi and G. Fekete and B. Szappanos and B. Kégl and B. Papp and C. Pál, Genome-wide analysis captures the determinants of the antibiotic cross-resistance interaction network, *Nat. Commun.* 5 (2014) 1–12. doi:10.1038/ncomms5352.
- 975
- [56] M. Dudeck, T. Horan, K. Peterson, K. Allen-Bridson, G. Morrell, A. Anttila, D. Pollock, J. Edwards, National healthcare safety network report, data summary for 2011, device-associated module, *Am. J. Infect. Control* 41 (2013) 286–300.
- 980
- [57] L. Mody, S. Maheshwari, A. Galecki, C. Kauffman, S. Bradley, Indwelling device use and antibiotic resistance in nursing homes: Identifying a high-risk group, *J. Am. Geriatr. Soc.* 55 (2007) 1921–1926.
- [58] B. Hota, Contamination, Disinfection, and Cross-Colonization: Are Hospital Surfaces Reservoirs for Nosocomial Infection?, *Clin. Infect. Dis.* 39 (2004) 1182–1189.
- 985
- [59] N. Cimolai, MRSA and the environment: implications for comprehensive control measures, *Eur. J. Clin. Microbiol. Infect. Dis.* 27 (2008) 481–493.

- [60] M. Maclean and K. McKenzie and S. Moorhead and R. Tomb and J. Coia
990 and S. MacGregor and J. Anderson, Decontamination of the Hospital En-
vironment: New Technologies for Infection Control, *Curr. Treat. Options*
Infect. Dis. 7 (2014) 39–51.
- [61] J. Han and N. Sullivan and B. Leas and D. Pegues and J. Kaczmarek
995 and C. Umscheid, Cleaning Hospital Room Surfaces to Prevent Health
CareAssociated Infections: A Technical Brief, *Ann. Intern. Med.* 163 (2015)
598–634.